



In situ rheological characterisation of wastewater sludge: comparison of stirred bioreactor and pipe flow configurations

Isabelle Seyssiecq, Mohsen Karrabi, Nicolas Roche

► To cite this version:

Isabelle Seyssiecq, Mohsen Karrabi, Nicolas Roche. In situ rheological characterisation of wastewater sludge: comparison of stirred bioreactor and pipe flow configurations. The Chemical Engineering Journal, 2015, 259, pp.205-212. <10.1016/j.cej.2014.07.102>. <hal-01467179>

HAL Id: hal-01467179

<https://hal.science/hal-01467179v1>

Submitted on 2 Mar 2023

HAL is a multi-disciplinary open access archive for the deposit and dissemination of scientific research documents, whether they are published or not. The documents may come from teaching and research institutions in France or abroad, or from public or private research centers.

L'archive ouverte pluridisciplinaire **HAL**, est destinée au dépôt et à la diffusion de documents scientifiques de niveau recherche, publiés ou non, émanant des établissements d'enseignement et de recherche français ou étrangers, des laboratoires publics ou privés.



HAL Authorization

In situ rheological characterisation of wastewater sludge: Comparison of stirred bioreactor and pipe flow configurations

Isabelle Seyssiecq^{*}, Mohsen Karrabi, Nicolas Roche

AMU – Aix Marseille Université, CNRS, LM²P², UMR 7340, Europôle de l'Arbois, Bâtiment Laënnec, Hall C, BP 80, 13545 Aix-en-Provence Cedex, France

In the present work, non-Newtonian properties of activated sludge are investigated using a bench test device specially developed for the purpose of this work. This set-up consists in a bioreactor equipped with a helical ribbon impeller (HRI configuration), and a recirculation loop of the sludge (pipe flow (PF) configuration). The HRI configuration is equipped with a motor and a torque-meter allowing *in situ* determination of sludge rheogram under stirred reactor conditions. On the PF configuration, differential pressure and flow transducers are implemented, allowing *in situ* determination of sludge rheogram under piping conditions. Both configurations are then compared. The yield stress, flow and consistency indexes of sludge suspensions (Herschel–Bulkley rheological law coefficients, τ_y , K and n) are determined over a large range of total suspended solid (TSS) concentrations, (12–38 g L⁻¹) in the laminar flow regime.

The analysis of experimental data shows that measurements performed with the PF configuration have to be corrected in order to take into account a wall slip phenomenon. A correction model is proposed that shows that slip mechanism is mostly due to wall static depletion at low solid concentrations (12–17 g L⁻¹), then turns to shear induced migration effect at higher solid concentrations (26–38 g L⁻¹).

1. Introduction

Biological processes such as classical activated sludge treatment or membrane bioreactors (MBR) have been broadly used for the treatment of wastewater within the last three decades. In recent years however, we are witness to an increase of global inflows entering wastewater treatment plants (WWTP), whereas authorised levels of pollutants in the outflows get more and more reduced. To face this context, WWTP new units have to become more and more efficient and a great attention is now paid to the

optimisation of treatment processes of both wastewater and excess wastewater sludge.

Important steps of treatment processes, notably on an economical point of view, but also as far as the yield of removal in pollutants is concerned are, aeration, settling or dewatering of biological sludge suspensions. The yield of each of these steps is directly linked to the flow or rheological properties of sludge suspensions that are involved. However, this link is complex and depends on a great number of parameters, such as biological or physico-chemical characteristics of the sludge, but also process operating conditions. As a consequence, the link between the yield of treatment processes and sludge suspensions rheological behaviour is still not clearly established.

This is notably due to the fact that in most of the previous studies, flow properties of sludge suspensions are measured after sampling, using a classical laboratory *ex situ* rheometer [1–9]. It follows that; rheological characterisation is performed under experimental conditions often far from the one prevailing in the process, notably

Abbreviations: CC, concentric cylinder; DCC, double concentric cylinder; HB, Herschel–Bulkley; HRI, helical ribbon impeller configuration; MBR, membrane bioreactor; P1, pipe one; P2, pipe two; PF, pipe flow configuration; ST, shear-thinning; SU, structural units; TSS, total suspended solids; VP, viscoplastic.

^{*} Corresponding author. Tel.: +33 491 289 302; fax: +33 491 289 402.

E-mail address: isabelle.seyssiecq@univ-amu.fr (I. Seyssiecq).

Nomenclature

a	constant for the slip velocity power law ($\text{m s}^{-1} \text{Pa}^{-m}$)
d	helical ribbon diameter (m)
D_h	hydraulic diameter of the pipe (m)
k_p	constant for N_p vs Re^{-1} in the laminar region for Newtonian fluids (–)
k'_p	constant for N_p vs Re_m^{-1} in the laminar region for non Newtonian fluids (–)
K	fluid consistency (Pa s^n)
K_{MO}	Metzner-Otto constant (–)
K_τ	Torque constant (Pa/Nm)
L	pipe length (m)
m	exponent for the slip velocity law (–)
n	fluid index (–)
N	rotation rate of the helical ribbon impeller (s^{-1})
N_p	power number (–)
Q	apparent volumetric flow rate (m^3/s)
Q_s	slip volumetric flow rate (m^3/s)
Q_t	true volumetric flow rate (m^3/s)
P	Power (W)

R	pipe radius (m)
Re	rotational Reynolds number (–)
Re_m	modified Reynolds number (–)
T	agitation torque (Nm)
TSS	total suspended solid concentration (g L^{-1})
U_s	slip velocity (m/s)

Greek letters

$\dot{\gamma}$	shear rate (s^{-1})
$\dot{\gamma}_a$	apparent shear rate (s^{-1})
$\dot{\gamma}_{MO}$	effective Metzner-Otto shear rate (s^{-1})
η	apparent viscosity (Pa s)
ΔP	pressure drop (Pa)
ρ	sludge density (kg m^{-3})
τ	shear stress (Pa)
τ_y	yield stress (Pa)
τ_w	wall shear stress (Pa)

in terms of the geometrical configuration in which flow of the sludge occurs. The geometrical parameter has though been shown to influence the result of the rheological characterisation of activated sludge [10].

Furthermore, as sludge is a biological material exhibiting a large range of rheological complexities such as shear-thinning behaviour, viscoplasticity, thixotropy or viscoelasticity [11,12], it can show important variations in behaviour (notably with time, shear or storage conditions). This latter point can also directly affect the response of the material to a given rheological measurement. As a result, although there are a large number of studies devoted to the rheological study of biological sludge suspensions [11–13], there is still a lot to do in this field, in particular to clear up the link between the configuration of the flow and the measured response in terms of rheological properties.

Activated sludge suspensions are known to be mainly composed of water, microorganisms and macromolecules aggregated in bioflocs. Bioflocs structure forms due to the phenomenon known as bioflocculation which can lead to a gel-like structure [14].

This aggregated structure depends on many factors and can evolve, notably when submitted to a shear stress. Such an aggregated internal structure is shared by a lot of concentrated dispersions of particles, droplets, bubbles or macromolecules and has been described in a very useful manner by Quemada [15], introducing the concept of Structural Units (SU). According to this concept, small primary elements can form larger groups (clusters, aggregates, flocs, clusters of flocs...). These groups are called SU and have a size which depends on the applied shear through the hydrodynamic stress acting on these structures. In most of the cases, when the dispersion is sheared, SU size is reduced, resulting in a release of trapped water and thus to an increase in fluidity of the material. This mechanism explains the shear-thinning (ST) properties that are generally observed in concentrated dispersions, such as wastewater sludge for values of solid concentration ranging from those prevailing in aeration basins (a few g L^{-1}) to much higher values [8,11,12]. In the same way, at sufficiently high solid content, a three dimensional network can form at rest between aggregated structures. A certain amount of shear stress will then need to be exceeded to overcome the force of this network and induce the flow of the material (viscoplastic behaviour = VP). This is notably the case with sufficiently concentrated wastewater sludge suspensions that are well known to behave like yield stress

fluids starting from values of solid concentration of around 10 g L^{-1} depending on many parameters such as the biopolymer composition, microorganisms type etc... [10–12,16]. At sufficiently high TSS, the shearing of complex internal structures of biological sludge will also lead to large scale time evolution i.e. thixotropy [17,18] or viscoelasticity [19–21].

In this study, we are interested in the flow behaviour of sludge suspensions in WWTP units, i.e. sheared suspensions under steady state flow. For this reason, only the steady state flow properties of sludge suspensions are taken into consideration.

In the range of TSS studied, the sludge shows both ST and VP behaviour and the Herschel–Bulkley model (Eqs. (1) and (2)) can be used to represent the rheogram or the viscosity curve of sludge suspensions:

$$\tau = \tau_y + K\dot{\gamma}^n \quad (1)$$

$$\eta = \frac{\tau_y}{\dot{\gamma}} + K\dot{\gamma}^{n-1} \quad (2)$$

where τ_y (Pa) is the yield stress, K (Pa s^n) the consistency index and n (–) the flow index.

In 2008, Mori et al. [10] carried out *ex situ* experiments on activated sludge with three different geometries: a helical ribbon impeller (HRI), a concentric cylinder (CC) and a double concentric cylinder (DCC) in cups. They studied the effect on the rheological behaviour of sewage sludge of measuring geometries at different biomass content ($4\text{--}43 \text{ g L}^{-1}$) and concluded that the geometry of measuring device influences the measured rheological properties.

The pipe flow configuration is, on a process point of view, a frequently encountered flow geometry (pumping lines of sludge between different tanks of the WWTP). As a consequence, the knowledge of sludge apparent viscosities in such a configuration could be of great help to the engineers, in order to perform the scale up of these lines.

Despite this fact, this flow configuration has almost never been used to investigate the rheological properties of biological suspensions [22]. Moreover, a comparison of results obtained, on a given sludge, with this type of configuration and more conventional configurations, such as the ones previously cited, has never been proposed.

In such a context, this work focussed on the characterisation of wastewater sludge rheological behaviour in the laminar region

(TSS concentration range from 12 to 38 g L⁻¹) with two completely different geometrical systems: a pipe flow (PF) configuration and a stirred (HRI) bioreactor. The rheological measurements are performed under *in situ* conditions, without any sampling of the material and in configurations close to the one prevailing in the process (pumping lines and agitated tanks). The aim is to demonstrate if the configuration of flows can affect the result of the rheological characterisation. The range of TSS chosen both allows sufficiently accurate *in situ* measurements and to cover the range of processes from MBR to flotation units.

In the case of both configurations, using the Herschel–Bulkley equation for modelling purposes, the yield stress but also flow and consistency indexes are determined in the whole range of biomass concentration, in laminar flow regime.

2. Materials and methods

2.1. sludge suspensions

The activated sludge used is sampled in a municipal (urban) WWTP (Aix en Provence City, 165.000 eq.inh., France) whose biomass concentration is about 4 g L⁻¹ in the recirculation loop between the secondary settlers and aeration basins. The range of concentration studied in this work is about 12 to 38 g L⁻¹. In order to obtain a fixed biomass content, the sample is first concentrated under gentle gravimetric filtration (no depression used to accelerate the process) using simple coffee filters (average pores diameters around 100 µm) and then diluted again with supernatant liquid. This method of concentration also used in previous works [6,10] has been shown not to affect the flocs structure.

2.2. Experimental set-up

The experimental set-up developed in this study is described schematically in Fig. 1. This set-up is mainly composed of two parts: a bioreactor and a recirculation loop. The double envelope bioreactor is 20 cm in height with an internal diameter of 11 cm. The liquid height is 19 cm, so that the working volume is 1.8 L.

It is equipped with a simple Helical Ribbon Impeller (HRI) rotating rather close to the wall ($d/D = 0.86$). Thus in all experiments presented in this paper, due to the high pumping capacity of the HRI [23] the sludge is flowing, even at the smallest rotation speed, and even in the far corners of the vessel (no dead zones).

Table 1

Geometrical characteristics of the experimental setup and operational conditions applied in this study.

Parameter	Unit	Notation	Pipe N°1	Pipe N°2	Bioreactor
Material	---	---	PVC	PVC	Plexiglas
Internal diameter	mm	D	17	13.6	110
Length	m	L	1	0.5	---
Liquid height	mm	H	---	---	190
HRI height	mm				95
Ribbon width	mm				10
Bottom clearance	mm				45
Ribbon pitch	mm				47.5
Flow rate	l/h	Q	200–700	200–700	---
Velocity	m/s	V	0.3–0.85	0.5–1.35	---
Reynolds number	---	Re	10–550	50–1000	<1
Temperature	°C	T	20	20	20

This remark justifies the subsequent assumptions made on the steadiness of the average shear rate and shear stress in the reactor.

The other geometrical parameters of the HRI are summarised in more details in Table 1.

In order to maintain a constant temperature of 20 °C (± 0.2 °C) within the effective volume of the bioreactor, the double envelope is connected to a thermostatic bath which allows water to circulate at an adjustable temperature. The Impeller is connected to a rheometer (Rheomat RM200) allowing measurements of the shear stress for different shear rates. The other part of the measurement system includes first a PVC tubular pipe of 1 m in length and 17 mm of internal diameter (pipe 1) followed by the second PVC pipe of 0.5 m in length and 14 mm of internal diameter (pipe 2). A rotary pump equipped with a speed controller is used to circulate the sludge through the pipes at different flow rates. The rotary pump is placed after the pipes so that the sludge structure is less affected by the passage through the pump. The stability with time of the values measured by the pipes indicates that the sludge structure is steady despite the passage through the pump. An electromagnetic flow meter device is used to measure the flow rates in the range 3.3 to 9.2 L/min. Two differential pressure transducers are set on each pipe to monitor pressure drops across the pipes.

An online data acquisition system is used to record different parameters as a function of time, such as the temperature, the torque and shear rate for the HRI system as well as pressure drops and volumetric flow rates for the PF system. Since the pipes are not regulated in temperature, it has been verified that the variation

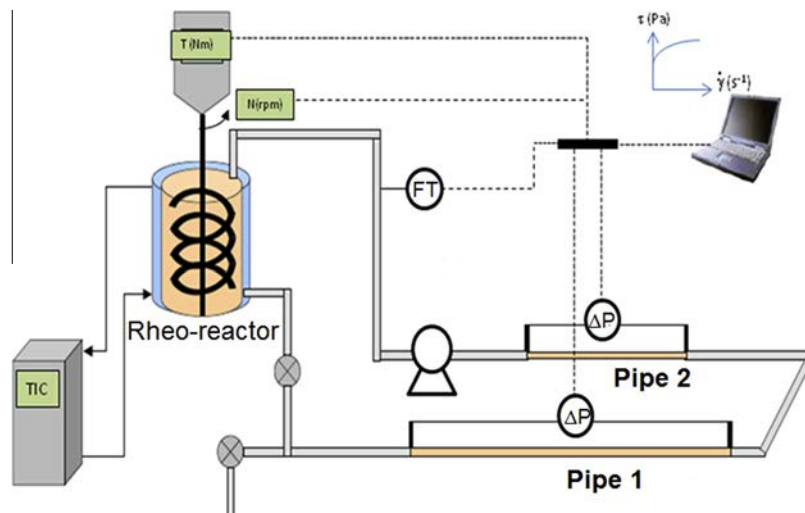


Fig. 1. Schematic representation of the experimental set-up.

in temperature is not significant between the entrance and the exit of the pipes (circulation times in pipes of only a few seconds).

The main specifications of the experimental set-up are given in Table 1.

2.3. Calculations

2.3.1. HRI system

In order to calibrate the HRI system for the viscosity curves or rheograms measurements, the hydrodynamic coefficients of the impeller have first to be determined using the Metzner–Otto principle [24]. This method has extensively been used to estimate the effective shear rate and shear stress in agitated reactors [25,26]. According to this method, an expression (in the laminar flow region) can be defined to represent the apparent viscosity (η_a), using the relation existing between the rotational Reynolds number $Re = \rho N d^2 / \eta$ and the dimensionless power number, $N_p = P / \rho N^3 d^5$, in a mechanically stirred reactor. Where the Power P can be calculated on the basis of the resistant torque (T) of the fluid ($P = 2\pi N T$), given that the rheometer (RM200) has first been calibrated in the air at different rotation speeds:

$$N_p = k_p \cdot Re^{-1} \quad (3)$$

where k_p is a dimensionless constant function of the impeller geometry for any Newtonian fluid [27]. This method can also apply to find out the corresponding constant, k'_p , in the case of a shear thinning fluid (Eq. (3)) using the modified Reynolds number, $Re_m = \rho N^{2-n} d^2 / K$. The effective shear rate $\dot{\gamma}_{MO}$ (s^{-1}) and shear stress τ (Pa) are defined as follows:

$$\dot{\gamma}_{MO} = K_{MO} N \quad (4)$$

$$\tau = K_\tau T \quad (5)$$

The K_{MO} constant is the Metzner–Otto dimensionless constant calculated from the Metzner–Otto principle [24,28].

From this principle, it can easily be demonstrated that $K_{MO} = (k_p/k'_p)^{1/n-1}$.

Then the torque constant can be deduced from the following relationship.

From Eq. (3) we deduce:

$$\frac{2\pi N T}{\rho N^3 d^5} = \frac{k_p \eta_e}{\rho N d^2} \rightarrow \eta_e = \frac{2\pi T}{k_p N d^3} \quad (6)$$

$$\tau = \eta_e \dot{\gamma}_{MO} = \eta_e K_{MO} N = \frac{2\pi K_{MO} T}{k_p d^3}$$

By comparing this latter relationship with Eq. (5), it follows that $K_\tau = 2\pi K_{MO} / k_p d^3$, is the proportionality constant between the shear stress and the torque (T).

The Metzner–Otto method has been widely used in chemical engineering researches to estimate the average shear rate in

agitated vessels [29–32]. However, it makes approximates, considering that the K_{MO} and K_τ values are constant, even in a non-Newtonian media.

For a more complete discussion on this point, the reader can refer to a work of 2008 [24] in which the validity of this assumption for identical sludge suspensions in an experimental device closely similar to the stirred reactor used in this work has been experimentally verified.

For the purpose of the HRI constants calibration, a Newtonian reference fluid (aqueous solution of glycerol, 96% in volume) as well as a non-Newtonian reference fluid (aqueous guar solution, 1% in wt) are used at 20 °C. Average values of 170 ± 10 (–) and 23.3 ± 1.2 (–) are respectively obtained for k_p and K_{MO} constants of the HRI system. This corresponds to a K_τ constant of 1004 ± 100 (Pa/Nm).

To validate those values, a comparison between the rheograms obtained with the HRI and a classical coaxial cylinders rheometer (AR550, TA instrument) has first been performed for each fluid that has been used in this study. The results obtained for reference fluids are shown in Fig. 2. In the case of sludge suspensions, those results do not appear on Fig. 3 for clarity purposes but they are mentioned in the following discussion section.

A comparison of the values obtained for the k_p and the K_{MO} constants with values calculated using literature correlations has also been performed. In the case of the K_{MO} constant, we can refer to the correlation of Shamlou-Ayazi [33] that gives a calculated value of 26.8 in the case of our helical ribbon and reactor, to see that our experimental value is in reasonable agreement.

In the case of the k_p constant, the correlation proposed by Kappel et al. [34] gives for our helical ribbon and reactor a calculated value of 182 which is also in good agreement with the experimental value.

Once bioreactor rheograms $\tau(\dot{\gamma}_{MO})$ have been drawn, modelling is performed for each TSS concentration using the HB model. HB parameters are determined using an iteration calculation (Matlab® program) that has been described in details in a previous paper [6].

2.3.2. Pipe flow system

Pipe flow viscometers have been used for rheological characterisation in lots of studies [11,12,22,35–38], among which some have been conducted on biological suspensions [22]. In the system studied here, the applied volumetric flow rate (Q) and the measured pressure drop (ΔP) are used to calculate the apparent shear rate $\dot{\gamma}_a$ and the wall shear stress (τ_w) using the following expressions:

$$\tau_w = D_h \cdot \Delta P / 4L \quad (7)$$

where D_h is the hydraulic diameter of the pipe taken as the internal diameter and ΔP is the pressure drop along the pipe length L .

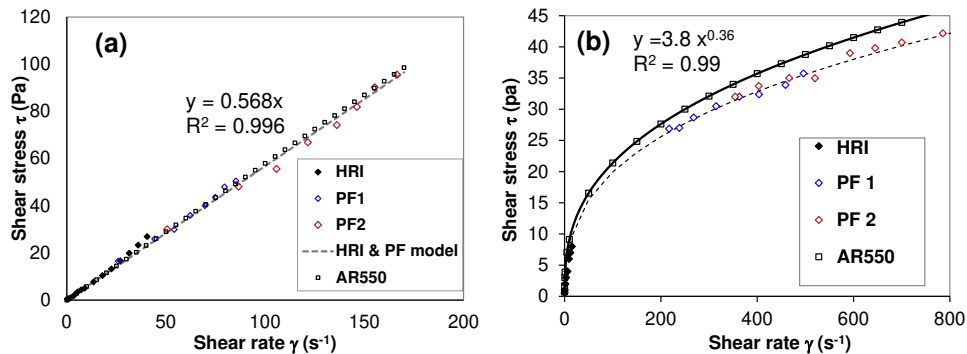


Fig. 2. Rheograms of (a) a newtonian fluid (aqueous solution of glycerol) and (b) a shear-thinning fluid (guar solution) using rheometer AR550 and both HRI and PF configurations.

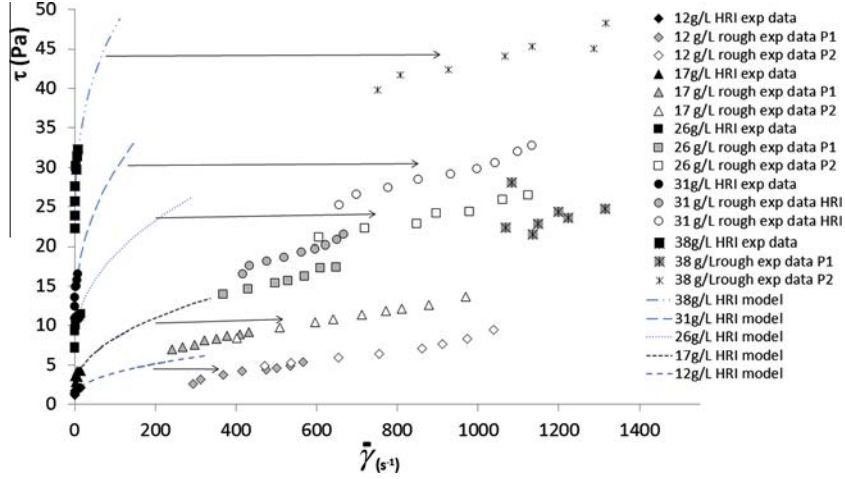


Fig. 3. Experimental measurements obtained in the HRI configuration (black filled symbols) and in the PF configuration for the pipe 1 (P1: grey filled symbols) and the pipe 2 (P2: white filled symbols).

Using the Rabinowitch-Money method, we obtain (Eq. (8)):

$$Q = \frac{\pi D_h^3}{8 \tau_w^3} \int_{\tau_y}^{\tau_w} \tau^2 \dot{\gamma}(\tau) d\tau \quad (8)$$

and considering the Herschel-Bulkley model for the rheological behaviour of sludge suspensions ($\dot{\gamma}(\tau) = (\frac{\tau - \tau_y}{K})^{1/n}$), we can deduce the following equation:

$$Q = \frac{\pi D_h^3}{8} \frac{n}{3n+1} \left(\frac{\tau_w - \tau_y}{K} \right)^{\frac{1}{n}} \left[1 - \frac{1}{2n+1} \left(\frac{\tau_y}{\tau_w} \right) - \frac{2n}{(2n+1)(n+1)} \left(\frac{\tau_y}{\tau_w} \right)^2 - \frac{2n^2}{(2n+1)(n+1)} \left(\frac{\tau_y}{\tau_w} \right)^3 \right] \quad (9)$$

which leads to the following definition for the Herschel-Bulkley apparent shear rate:

$$\dot{\gamma}_a = \left(\frac{\tau_w - \tau_y}{K} \right)^{\frac{1}{n}} = \frac{8Q}{\pi D_h^3} \frac{3n+1}{n} \times \left(\frac{1}{\left[1 - \frac{1}{2n+1} \left(\frac{\tau_y}{\tau_w} \right) - \frac{2n}{(2n+1)(n+1)} \left(\frac{\tau_y}{\tau_w} \right)^2 - \frac{2n^2}{(2n+1)(n+1)} \left(\frac{\tau_y}{\tau_w} \right)^3 \right]} \right) \quad (10)$$

The calculation of the apparent shear rate from Eq. (9) is performed using for the values of the HB model parameters τ_y and n , values obtained with the bioreactor configuration that are used as a reference (see discussion here-after).

The calculations presented here-above for the PF system allow drawing pipe flow raw rheograms $\tau_w(\dot{\gamma}_a)$ that are discussed in the following part.

Once some of the rheograms obtained with sludge suspensions have been corrected for slip effects (PF systems), modelling is performed for data obtained with both configurations and for each TSS concentration using the HB model. HB parameters are still determined using the Matlab® iteration program [6].

3. Results and discussion

3.1. Calibration with reference fluids

The set-up has first been calibrated using a Newtonian reference fluid composed of an aqueous solution of glycerol 94% in volume (Fig. 2(a)) and a shear-thinning reference fluid consisting in a 1% in weight aqueous solution of guar (Fig. 2(b)). The Fig. 2 shows

the ability of HRI and PF configurations to accurately characterise the rheological properties of both Newtonian and shear-thinning single phase fluids.

Concerning the Newtonian fluid, we can observe that the results approximately indicate the same viscosity of 568 mPa s for HRI and PF systems which is close to the value measured with a classical coaxial cylinders rheometer (AR550, TA instrument) (580 mPa s for a 94% in volume glycerol solution at 20 °C) (Fig. 2(a)). We can see that the different systems allow covering very different ranges of shear rates. The HRI system works in the lower range of shear rates (0–50 s⁻¹), the pipe 1 (P1) works in an intermediate range (50–100 s⁻¹) and the pipe 2 (P2) in the upper range of shear rates (60–180 s⁻¹).

Concerning the shear-thinning reference fluid, Fig. 2(b) also shows that all three systems measure identical rheological properties for this fluid. Indeed, the same shear thinning behaviour modelled by an Ostwald power law with a consistency index of 3.8 Pa sⁿ and a flow index of 0.36 is found for this solution whatever the measurement system over the global shear rate range 0–900 s⁻¹. Closely identical values ($K = 3.89 \text{ Pa s}^n$ and $n = 0.37$) of the power law model coefficients have been confirmed with this guar solution at 20 °C, using a classical coaxial cylinders rheometer measurement (AR550, TA instrument) in the same shear rate range. This measurement also appears on Fig. 2(b).

This set-up can now be used to perform the *in situ* rheological characterisation of wastewater sludge suspensions with solid contents ranging from 12 to 38 g L⁻¹ in TSS using HRI and PF configurations (P1 and P2).

3.2. Measurements with sludge suspensions

3.2.1. Raw measurements

Fig. 3 shows the raw data obtained with the 12/17/26/31 and 38 g L⁻¹ sludge suspensions (data measured with the HRI represented by black filled symbols, data measured with the P1 system represented by grey filled symbols and data obtained with the P2 system represented by empty symbols).

The dotted lines represent the Herschel-Bulkley model that best fits the data obtained with the HRI system.

It has been verified for each solid concentration, that this HRI extrapolated flow curve is in good agreement with the AR550 measurement.

It can be observed in Fig. 3 that, in the case of sludge suspensions, the raw results obtained with the HRI system on one side

and the PF systems on the other side are no more consistent. In particular, the data calculated for the PF systems seem to be shifted to higher shear rates (see arrows on Fig. 3) when compared to what should be expected on the basis of the HRI measurements (dotted lines giving the HRI flow curve extrapolated at higher shear rates).

The apparent drop in viscosity observed with pipes could be explained by a wall slip effect. It is indeed well known that, working with complex fluids in all kind of rheometers, a slip phenomenon can develop at the wall. The slip is known to be particularly acute in the case of geometries giving rise to a shear stress gradient away from the wall, as for instance capillary tubes [39,40].

On the contrary, the HRI system is a stirring type rheo-reactor and could be qualified as a “no slip” reference system (often referred as a vane system in articles) [39,40].

For this reason, in this work the flow curve that is calculated on the basis of the HRI experiments and extrapolated at higher shear rates will be used as a “no slip” reference flow curve for the pipe flow experiments.

The slip phenomenon has been widely described in lots of articles [39–45] and is known to be due to a drop in solid concentration close to the moving geometry or close to the wall in the case of pipes. The presence of a less concentrated thin layer of lower viscosity close to the wall induces, for a given shear stress a local enhancement of the shear rate. The rest of the suspension, still at the average bulk concentration remains normally sheared but slips onto this liquid thin layer.

It follows that the observed shear rate is bigger than the shear rate corresponding to a homogeneous shearing of the suspension.

In order to correct flow measurements for slip, the calculation of slip velocities is generally performed by comparing the results obtained for a similar shear stress with geometries of different sizes (capillary tubes of different internal diameters).

In the case of this study, the experimental set-up is equipped with tubes of two different diameters. However, it is not possible to cover an identical range of shear stresses with pipe 1 and pipe 2. This is due to the fact that experiments are limited by the pump to a certain range of volumetric flow rates that corresponds to very different shear rates and thus shear stresses ranges when the suspension flows from pipe 1 to pipe 2. It is thus not possible here, to compare data obtained with pipe 1 and pipe 2 and calculate the slip velocities.

The correction for slip of raw data obtained with pipe 1 and 2 will thus be done by referring to the “no slip” reference flow curve (HRI) and deduce, for a given TSS concentration, slip velocities that allow corrected data from either pipe 1 and pipe 2 to overlap with this reference curve.

3.2.2. Slip corrected measurements

The correlation for slip proposed by Cohen & Metzner [41,42] for a power law Ostwald fluid can be adapted for a viscoplastic Herschel–Bulkley fluid. This leads to the following equation for the slip volumetric flow rate (Q_s) as a function of the apparent volumetric flow rate (Q):

$$Q_s = \frac{Q}{1 + \left(\frac{\tau_y - \tau_w}{K} \right)^{1/n} \frac{R}{a(\tau_w)^m} \frac{n}{3n+1} \left[1 - \frac{1}{2n+1} \left(\frac{\tau_y}{\tau_w} \right) - \frac{2n}{(2n+1)(n+1)} \left(\frac{\tau_y}{\tau_w} \right)^2 - \frac{2n^2}{(2n+1)(n+1)} \left(\frac{\tau_y}{\tau_w} \right)^3 \right]} \quad (11)$$

In Eq. (11), the apparent volumetric flow rate (Q) is taken as the sum of the slip flow rate (Q_s) and the true flow rate (Q_t); $\left(\frac{\tau_y - \tau_w}{K} \right)^{1/n}$ in which τ_y , K and n are determined on the basis of the HRI experimental points, using the Herschel–Bulkley model, represents the true shear rate and $\frac{R}{a(\tau_w)^m} \frac{n}{3n+1} \left[1 - \frac{1}{2n+1} \left(\frac{\tau_y}{\tau_w} \right) - \frac{2n}{(2n+1)(n+1)} \left(\frac{\tau_y}{\tau_w} \right)^2 - \frac{2n^2}{(2n+1)(n+1)} \left(\frac{\tau_y}{\tau_w} \right)^3 \right]$ represents the opposite of the slip shear rate.

The slip velocity is taken as an empirical power function of the wall shear stress according to Eq. (12):

$$U_s = a(\tau_w)^m \quad (12)$$

In Eq. (12), no critical shear stress for the appearance of slip is taken into consideration on the contrary of Chen et al. in their study of the slip flow of coal water slurries [43]. This is justified by the fact that, in the case of the sludge suspensions tested here, slip may be observed at even low shear stress as it will be discussed later on.

Parameters a and m are adjusted on experimental data for each TSS concentration, so that the corrected pipe flow measurements obtained for either pipe 1 and pipe 2 are the closest to the extrapolated HRI flow curve. The values obtained for a and m are then given in Table 2 together with the Herschel–Bulkley parameters of the corrected rheograms as a function of the TSS.

Fig. 4 shows the evolution of calculated slip velocities as a function of the wall shear stress for different solid concentrations. It is worth noting that these calculated slip velocity values are of the same order of magnitude than experimentally measured slip velocities in the case of suspensions published by Chen et al. [43,44].

Fig. 4 shows that slip velocities decrease with increasing solid concentrations, at a constant effective shear stress, but following different laws according to the solid concentration range.

The slip velocities of the two lowest solid concentrations (12 and 17 g L⁻¹) show a linear increase with the effective shear stress giving rise to high slip velocities values at even low shear stresses. This behaviour is known to be due to the formation of a slip layer under the control of static wall depletion effects. Indeed, close to the solid boundaries, the solid particles cannot occupy the space as efficiently as in the bulk of the suspension. This phenomenon leads to the formation of a liquid-rich layer adjacent to the wall which is present even under zero shear rate. It follows that the suspension will start to slip significantly onto this liquid-rich layer

Table 2
Model parameters obtained for different TSS concentrations.

TSS (g L ⁻¹)	Herschel–Bulkley model parameters			Slip velocity parameters	
	τ_y (Pa)	K (Pa s ⁿ)	n (–)	a (m Pa ⁻¹ s ⁻¹)	m (–)
12	1.13	0.3	0.49	0.09	1
17	1.7	0.81	0.46	0.05	1
26	7.1	1.49	0.45	0.015	1.2
31	9.5	2.9	0.42	0.014	1.2
38	21	5.1	0.36	0.0047	1.3

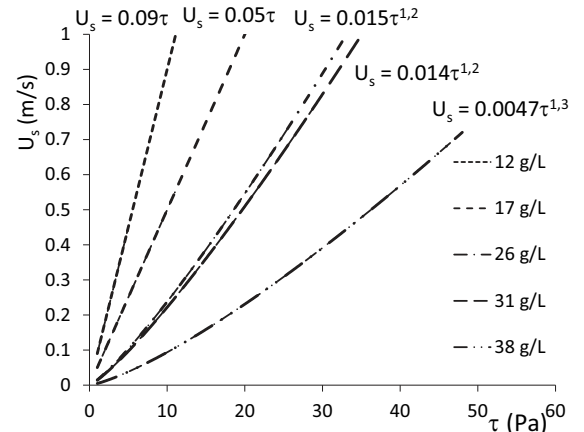


Fig. 4. Evolution of calculated slip velocities as a function of the wall shear stress for different TSS concentrations.

even at very low shear stresses. The linear increase of the slip velocity with the shear stress indicates that the slip layer keeps the same thickness and viscosity as the shear stress increases.

In the case of more concentrated suspensions ($26\text{--}38\text{ g L}^{-1}$), static wall depletion effects are not the only slip mechanism and the formation of the slip layer also begins to be affected by shear-induced particles migration effects. Above a certain concentration level, the addition of more solid particles induces a significant increase of inter-particles interactions. This phenomenon results in the appearance of a significant yield stress (τ_y) for these suspensions: 12 g L^{-1} suspensions have very small yield stresses $\tau_y = 1.13\text{ \& 1.7 Pa}$, whereas for $26/31\text{ \& }38\text{ g L}^{-1}$ suspensions, the yield stress value becomes significant with $\tau_y = 7.1/9.5\text{ \& }21\text{ Pa}$ respectively.

However, the addition of more and more solid particles also leads to an important increase in interactions between the bulk suspension and the walls, reducing in turn the thickness of the liquid-rich layer due to static wall depletion effects. If this layer becomes small compared to the roughness of the wall, significant slip can no more develop under low shear stresses. When the wall shear stress increases however, and becomes much larger than the yield stress of the suspension so that there is a significant shear deformation of the bulk suspension, a large number of particles begin to migrate from the wall to the centre of the pipe (bulk of the suspension), resulting in a shear-induced creation of a liquid-rich slip layer. This explains why the slip velocity increases with the shear stress according to a power law (Eq. (12)) with an exponent (m) being more and more important as the solid concentration increases.

It is also worth noting that the percentages of slip velocity with respect to the average fluid velocity are high varying from 50% (12 g L^{-1} sludge under the highest shear stress) to 99% (38 g L^{-1} sludge under the smallest shear stress).

This is in good agreement with results from Chen et al. [43] for slip flow of coal water slurries in pipelines obtained with particles of several hundreds of μm in diameter (sludge flocs have been estimated here at about $150\text{ }\mu\text{m}$ in mean diameter).

The slip corrected flow curves are presented on Fig. 5 for the three configurations: HRI (black filled symbols), pipe 1 (grey filled symbols) and pipe 2 (empty symbols).

The Herschel-Bulkley model parameters that best fit the experimental data, for the different biomass concentrations, are given in Table 2. They show classical variations with the TSS concentration

corresponding to an increase in both viscoplasticity and shear-thinning as the solid concentration increases.

It can also be observed that, for each TSS concentration, taking into account slip velocities on the basis of the values presented in Fig. 4 allow the experimental data obtained with both pipes to come rather close to the extrapolated HRI “no slip” reference flow curve.

The agreement between data obtained with the three different systems is however lower as the solid concentration increases.

4. Conclusions

In this study, we have measured rheological properties of wastewater sludge suspensions at different biomass contents ($12\text{--}38\text{ g L}^{-1}$) using two different systems (HRI and PF systems). A helical ribbon impeller in a stirred bioreactor coupled with a rheometer apparatus (RM 200) first allowed to *in situ* measure the rheological behaviour of activated sludge under stirred conditions. The pressure drop as well as the sludge flow rate recorded along the pipe line configurations (PF systems), also allowed direct calculations of the shear stress and shear rates at the wall for the sludge under pumping conditions.

Although both types of configurations can be used to accurately determine the rheogram of Newtonian or shear-thinning monophasic “simple” fluids, measurements performed with activated sludge suspensions are more complex to interpret.

The bioreactor HRI system allows performing measurements in a low shear rates range without any artefacts, provided that the constants of the system (K_τ & K_{MO}) have been accurately measured using calibration fluids and validated with measurements made with classical rheometer and geometry.

On the contrary, in the case of the PVC pipes that have been used in this work, the pipe flow systems, show an important wall slip phenomenon that needs to be subtracted from the raw results in order to determine the correct flow curve of activated sludge suspensions.

Taking the HRI extrapolated flow curve as a “no slip” reference curve, it was possible to calculate slip velocities so that the pipe flow curves can overlap with this reference curve.

The calculated slip velocities that are needed to correct these measurements are of the same order of magnitude than experimental slip velocities measured by other authors. They show variations with shear stress pointing out that slip by wall static

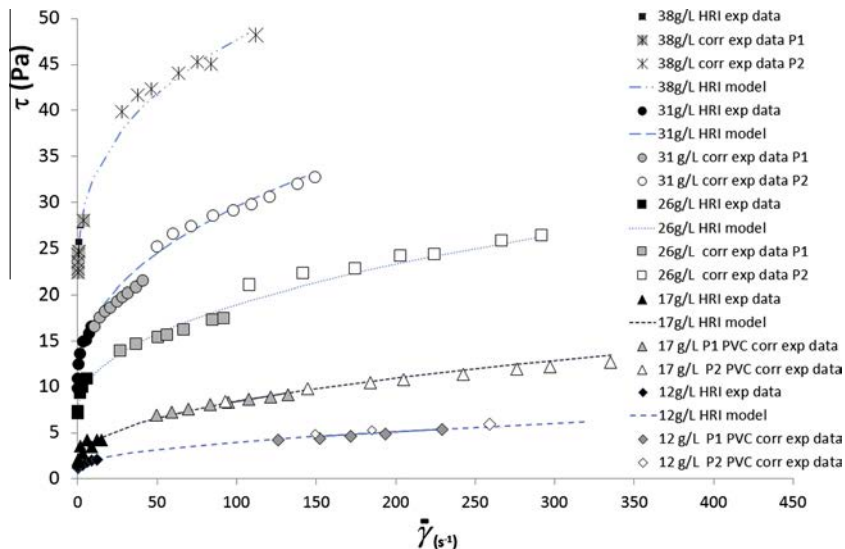


Fig. 5. Experimental measurements obtained in the HRI configuration (black filled symbols) and corrected data for the PF configuration for the pipe 1 (P1: grey filled symbols) and the pipe 2 (P2: white filled symbols).

depletion effect is the main slip mechanism for low solid concentrations suspensions (12 & 17 g L^{-1}).

When the solid concentration becomes sufficient for the solid phase to interact with the walls ($26\text{--}38 \text{ g L}^{-1}$), the main slip mechanism turns to a shear induced migration mechanism.

In the current state of development of our set-up, correction calculations that have been presented in this paper are needed to access the true rheological properties of sludge suspensions from the pipe line configurations. However, the simplest experimental method to reduce slip (whatever the measuring geometry is) consist in increasing the wall roughness, so that it becomes large enough compared to the material structural units (SU) size (flocs size in the case of sludge) for the SU concentration to be kept constant between the wall and the bulk and thus avoid slip by static wall depletion.

The pipes used in this work are made of PVC because it is a low cost material easy to work with. However, it is also a very low roughness material (only a few μm) that will, as a consequence, be very sensitive to wall slip appearance.

One of the prospects of this work is to equip our set-up with high roughness pipes made of rough steel for example. In this way, the wall roughness could be increased to the same order of magnitude than the solid particles size (sludge flocs about $150 \mu\text{m}$ in mean diameter here), so that the slip at the wall could be reduced. An increase in wall roughness should indeed at least avoid slip phenomena that are due to wall static depletion effects and allow direct measurements of the true rheological properties for sludge suspensions with the smaller TSS, for which the slip mechanism is supposed to be mainly due to such static depletion effects.

Acknowledgements

The authors are indebted to the Carnot STAR Institute (Aix-Marseille University) and the French National Scientific Research Center (CNRS) for partial funding of this work.

References

- [1] L.H. Mikkelsen, The shear sensitivity of activated sludge. Relations to filterability, rheology and surface chemistry, *Colloids Surf. A* 182 (2001) 1–14.
- [2] P. Battistoni, P. Pavan, J. Mata-Alvarez, M. Prisciandaro, F. Cecchi, Rheology of sludge from double phase anaerobic digestion of organic fraction of municipal solid waste, *Water Sci. Technol.* 41 (2000) 51–59.
- [3] G. Moeller, L.G. Torres, Rheological characterization of primary and secondary sludges treated by both aerobic and anaerobic digestion, *Bioresour. Technol.* 61 (1997) 207–211.
- [4] V. Loiito, L. Spinosa, G. Mininni, R. Antonacci, The rheology of sewage sludge at different steps of treatment, *Water Sci. Technol.* 36 (1997) 79–85.
- [5] P.T. Slatter, The rheological characterisation of sludges, *Water Sci. Technol.* 36 (1997) 9–18.
- [6] M. Mori, I. Seyssiecq, N. Roche, Rheological characterisation of activated sludge, *Process Biochem.* 41 (2006) 1656–1662.
- [7] D.A. Grant, C.W. Robinson, Measurement of rheological properties of filamentous fermentation broths, *Chem. Eng. Sci.* 45 (1990) 37–48.
- [8] M.M. Sozanski, E.S. Kempa, K. Grocholski, J. Bien, The rheological experiment in sludge properties research, *Water Sci. Technol.* 36 (1997) 69–78.
- [9] R.I. Dick, B.B. Ewing, The rheology of activated sludge, *J. Water Pollut. Control Fed.* 39 (1967) 543–560.
- [10] M. Mori, I. Seyssiecq, J. Isaac, N. Roche, Effect of measuring geometries and of Exocellular Polymeric Substances on the rheological behavior of sewage sludge, *Chem. Eng. Res. Des.* 86 (2008) 554–559.
- [11] I. Seyssiecq, J.H. Ferrasse, N. Roche, State of the art: rheological characterisation of wastewater treatment sludge, *Biochem. Eng. J.* 16 (2003) 41–56.
- [12] N. Eshtiaghi, F. Markis, S. Dong Yap, J.C. Baudez, P. Slatter, Rheological characterisation of municipal sludge: a review, *Water Res.* 47 (2013) 5493–5510.
- [13] N. Ratkovich, W. Horn, F.P. Helmus, S. Rosenberger, W. Naessens, I. Nopens, T.R. Bentzen, Activated sludge rheology: a critical review on data collection and modelling, *Water Res.* 47 (2013) 463–482.
- [14] C.S. Laspidou, B.E. Rittmann, A unified theory for extracellular polymeric substances, soluble microbial products, and active and inert biomass, *Water Res.* 36 (2002) 2711–2720.
- [15] D. Quemada, Rheological modelling of complex fluids: I – the concept of effective volume fraction revisited, *Eur. Phys. J. Appl. Phys.* 1 (1997) 119–127.
- [16] S. Akkache, I. Seyssiecq, N. Roche, Effect of exo polysaccharide concentration on the rheological properties and Settling ability of activated sludge, *Environ. Technol. J.* 34 (2013) 2995–3003.
- [17] J.C. Baudez, Physical aging and thixotropy in sludge rheology, *Appl. Rheol.* 18 (2008) 13459–13466.
- [18] N. Tixier, G. Guibaud, M. Baudu, Determination of some rheological parameters for the characterization of activated sludge, *Bioresour. Technol.* 90 (2003) 215–220.
- [19] A. Ayol, S.K. Dentel, Enzymatic treatment effects on dewaterability of anaerobically digested biosolids II: laboratory characterizations of drainability and filterability, *Process Biochem.* 40 (2005) 2435–2442.
- [20] R.P. Chhabra, J.F. Richardson, *Non-Newtonian Flow and Applied Rheology, Engineering Applications*, second ed., Elsevier, 2008.
- [21] Y.L. Wang, S.K. Dentel, The effect of polymer doses and extended mixing intensity on the geometric and rheological characteristics of conditioned anaerobic digested sludge (ADS), *Chem. Eng. J.* 166 (2011) 850–858.
- [22] Y. Manon, D. Anne-Archard, J.L. Uribelarrea, C. Molina-Jouve, L. Fillaudeau, Physical and biological study of cell cultures in a bioreactor: on-line and off-line rheological analyses, *Appl. Rheol.* 21 (2011) 35167.
- [23] J.J. Ulbrecht, P.J. Carreau, Mixing of viscous non Newtonian liquids, in: J.J. Ulbrecht, G.K. Patterson (Eds.), *Mixing of Liquids by Mechanical Agitation*, Gordon & Breach, New York, 1985 (chapter 4).
- [24] A.B. Metzner, R.E. Otto, Agitation of non-Newtonian liquids, *AIChE J.* 3 (1957) 3–10.
- [25] I. Seyssiecq, B. Marrot, D. Djerrou, N. Roche, In-situ triphasic rheological characterisation of activated sludge, in an aerated bioreactor, *Chem. Eng. J.* 142 (2008) 40–47.
- [26] T.C. Nguyen, D. Anne-Archard, V. Coma, X. Cameleyre, E. Lombard, C. Binet, A. Nouhen, K. Anh To, L. Fillaudeau, In situ rheometry of concentrated cellulose fibre suspensions and relationships with enzymatic hydrolysis, *Bioresour. Technol.* 133 (2013) 563–572.
- [27] K. Rajeev, Ch. Thakur, G. Vial, M. Djelveh, M. Labbafi, Mixing of complex fluids with flat-bladed impellers: effect of impeller geometry and highly shear-thinning behavior, *Chem. Eng. Process* 43 (2004) 1211–1222.
- [28] H. Desplanches, J.L. Chevalier, *Mélange des milieux pâteux de rhéologie complexe. Théorie, Techniques de l'ingénieur*, 1999 (J3 860, 1–20).
- [29] A. Iranshahi, M. Heniche, F. Bertrand, P.A. Tanguy, Numerical investigation of the mixing efficiency of the Ekato Paravisc impeller, *Chem. Eng. Sci.* 61 (2006) 2609–2617.
- [30] L. Choplin, P. Marchal, mixer-type rheometry for food products. *Int. Symp. of Food rheology and structure I, Zurich* (1997) 40–44.
- [31] P.J. Carreau, J. Paris, P. Guerrin, Mixing of Newtonian and non-Newtonian liquids: screw agitator and draft coil system, *Can. J. Chem. Eng.* 70 (1992) 1071–1081.
- [32] J.M. Ducla, H. Desplanches, J.L. Chevalier, Effective viscosity of non-Newtonian fluids in a mechanically stirred tank, *Chem. Eng. Commun.* 21 (1986) 29–36.
- [33] P. Shamlou-Ayazi, *Heat transfer in mixing vessels at low Reynolds numbers* (Ph.D. thesis), Univ. Bradford U.K., 1980.
- [34] M. Kappel, H. Seibring, Power requirements and mixing time in agitation of high viscous liquids by the helical ribbons, *Verfahrenstechnik* 4 (10) (1970) 470–475.
- [35] Y. Cohen, (Ph.D. thesis), Univ. of Delaware, Newark, 1981.
- [36] B. Herzhaft, S. Kakadjian, M. Moan, Measurement and modeling of the flow behavior of aqueous foams using a recirculating pipe rheometer, *Colloids Surf. A* 263 (2005) 153–164.
- [37] C.S. Chen, S.C. Chen, W.L. Liaw, R.D. Chien, Rheological behavior of POM polymer melt flowing through micro-channels, *Eur. Polym. J.* 44 (2008) 1891–1898.
- [38] L. Pullum, P. Slatter, L. Graham, A. Chrysos, Are tube viscometer valid for suspension flows?, *Korea-Aust Rheol. J.* 22 (3) (2010) 163–168.
- [39] H.A. Barnes, A review of the slip (wall depletion) of polymer solutions, emulsions and particle suspensions in viscometers: its cause, character and cure, *J. non-Newtonian Fluid* 56 (1995) 221–251.
- [40] P. Coussot, *Rheometry of Pastes Suspensions and Granular Materials*, John Wiley & sons, Inc, 2005.
- [41] Y. Cohen, A.B. Metzner, Apparent slip flow of polymer solutions, *J. Rheol.* 29 (1985) 67–102.
- [42] Y. Cohen, A.B. Metzner, An analysis of apparent slip flow of polymer solutions, *Rheol. Acta* 25 (1986) 28–35.
- [43] L. Chen, Y. Duan, C. Zhao, L. Yang, Rheological behavior and wall slip of concentrated coal water slurry in pipe flows, *Chem. Eng. Process* 48 (2009) 1241–1248.
- [44] L. Chen, Y. Duan, L. Yang, C. Zhao, Slip flow of coal water slurries in pipelines, *Fuel* 89 (2010) 1119–1126.
- [45] R.G. Cox, S.G. Mason, Suspended particles in fluid flow through tubes, *Annu. Rev. Fluid Mech.* 3 (1971) 291–316.